



# Self-organized $\text{ZnAl}_2\text{O}_4$ nanostructures grown on *c*-sapphire

Justina Grabowska<sup>a</sup>, Karuna Kar Nanda<sup>a,1</sup>, R.T. Rajendra Kumar<sup>a</sup>,  
J.P. Mosnier<sup>a</sup>, M.O. Henry<sup>a</sup>, Simon B. Newcomb<sup>b</sup>, Patrick McNally<sup>c</sup>,  
Lisa O'Reilly<sup>c</sup>, Xu Lu<sup>c</sup>, Enda McGlynn<sup>a,\*</sup>

<sup>a</sup> School of Physical Sciences, NCPST, Dublin City University, Glasnevin, Dublin 9, Ireland

<sup>b</sup> Glebe Scientific Ltd., Newport, Co. Tipperary, Ireland

<sup>c</sup> School of Electronic Engineering/RINCE, Dublin City University, Glasnevin, Dublin 9, Ireland

## Abstract

Self-organized  $\text{ZnAl}_2\text{O}_4$  nanostructures with the appearance (in SEM) of high aspect ratio horizontal nanowires are grown on uncatalysed *c*-sapphire by vapour phase transport. The nanostructures grow as three equivalent crystallographic variants on *c*-sapphire. Raman and cathodoluminescence spectroscopy confirm that the nanostructures are not ZnO and TEM shows that they are the cubic spinel, zinc aluminate,  $\text{ZnAl}_2\text{O}_4$ , formed by the reaction of Zn and O with the sapphire substrate.

© 2007 Elsevier Ltd. All rights reserved.

**Keywords:** Zinc aluminate; Spinel; Epitaxy; Sapphire; Growth; SEM; TEM; Raman; Cathodoluminescence

## 1. Introduction

One-dimensional wide bandgap semiconductor nanostructures (NS) are the subject of research interest for application in photonic devices [1]. For example, vertical growth of ZnO nanowires is reported on different substrates by a variety of methods [2]. Growth of wide bandgap horizontal nanowires has been less successful to date with limited reports of such structures [3].

\* Corresponding author. Tel.: +353 1 7005387; fax: +353 1 7005384.

E-mail address: [enda.mcglynn@dcu.ie](mailto:enda.mcglynn@dcu.ie) (E. McGlynn).

<sup>1</sup> Present address: Materials Research Centre, Indian Institute of Science, Bangalore 560 012, India.

Controlled growth of NS is an important research topic because such structures can be used in many applications in nanotechnology.

We report growth of self-organized  $\text{ZnAl}_2\text{O}_4$  NS (with the appearance in scanning electron microscopy (SEM) images of high aspect ratio horizontal nanowires) on uncatalysed *c*-sapphire by vapour phase transport (VPT) in addition to polycrystalline  $\text{ZnAl}_2\text{O}_4$  layer deposition, via the reaction of Zn and O with the sapphire substrate. The NS grow as three equivalent crystallographic variants on *c*-sapphire. Under similar conditions of temperature/gas atmosphere, using a gold catalyst, vertical ZnO nanowires grow in our system, as reported previously [2,4].  $\text{ZnAl}_2\text{O}_4$  NS have applications in a variety of technologies including sensing and catalysis and the growth of NS with well defined orientation on sapphire substrates may offer advantages for e.g. catalytic reactions such as cracking, dehydration, hydrogenation, and dehydrogenation reactions [5].

## 2. Experimental methodology

NS were grown on *c*-sapphire by VPT. The substrates are *c*-plane sapphire, obtained mainly from Testbourne (<http://www.testbourne.com/>), and are ultrasonically cleaned before growth and are not generally patterned with gold. A ZnO/graphite powder mix (1:1 wt) is placed at one end of a quartz boat and the substrate is placed  $\sim 0.5$ – $5.0$  cm from the source in a single zone tube furnace with argon carrier flow (90 sccm). The nominal temperature of the furnace is set in the range  $950$ – $1125$  °C and the set temperature is achieved in  $\sim 15$ – $20$  min. The deposition time is  $30$ – $60$  min. Vapour–liquid–solid (VLS) growth [2] of vertical ZnO nanowires was achieved with similar conditions by depositing a gold layer of thickness  $\sim 2.0$  nm on the sapphire prior to growth. Samples were characterized by SEM (both LEO Stereoscan 440 & Hitachi S-4300 Field Emission), atomic force microscopy (AFM: Nanoscope IIIa, Digital Instruments; contact mode). Energy-dispersive x-ray (EDX) and cathodoluminescence (CL-SEM) were performed using an EDX spectrometer and Gatan Instruments CL coupled to the LEO Stereoscan SEM, respectively. Micro-Raman data were measured using a Jobin–Yvon LabRam 800 micro-Raman spectroscopy system with UV HeCd excitation. Transmission electron microscopy (TEM) was performed using a JEOL2000FX operating at 200 kV. Sections for microstructural evaluation were made using standard focused ion beam (FIB) thinning (see e.g. reference [6]). Laue pattern data were acquired at the Fluo–Topo x-ray topography beamline of the ANKA (Ångström Karlsruhe) at the Institute for Synchrotron Radiation (ISS), in Karlsruhe, Germany, using the continuous spectrum of synchrotron radiation from a 2.5 GeV storage ring at typical currents of  $100$ – $180$  mA. Details on Laue measurements are given in [7,8].

## 3. Results

A SEM image of NS grown at a nominal furnace temperature of  $950$  °C and a substrate temperature of  $915$  °C (growth duration 30 min), is shown in Fig. 1(a) and at higher magnification in Fig. 1(b). NS appear to grow as horizontal nanowires in *three* specific directions indicated by arrows with an angle of  $120^\circ$  between them and appear uniformly distributed among these directions. The apparent diameter of the majority of the NS is very close to 70 nm, though we observe diameters from 60 to 80 nm and lengths of  $400$ – $600$  nm. The NS appear nearly monodisperse in diameter. A SEM image of NS synthesized with a nominal furnace temperature of  $1125$  °C and a substrate temperature of  $1075$  °C (growth duration 30 min), is shown in Fig. 1(c). The apparent NS diameter is marginally greater at  $\sim 80$  nm with lengths in the range

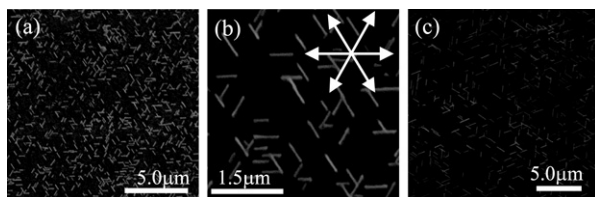


Fig. 1. SEM images of NS on *c*-sapphire; (a) growth temperature 900–950 °C; (b) higher magnification of sample in (a); (c) growth temperature ~1075 °C.

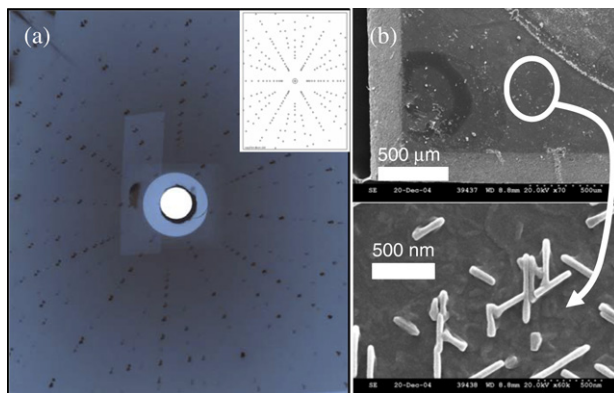


Fig. 2. (a) Laue pattern of *c*-sapphire, inset shows a simulated pattern used to orient sample; (b) SEM data showing orientation of NS with respect to sample edges.

of 700–1500 nm. We performed atomic force microscopy (AFM) on these samples (not shown). The average height of the NS is ~70 nm. AFM profiles along the long axis of most NS indicates that for reasonably long NS the change in height is less than ~5 nm over the NS length of ~800 nm. EDX (not shown) shows the chemical composition of regions with NS to be Zn, Al and O, as expected.

The relative orientation of the NS on the *c*-sapphire surfaces was studied using a Laue pattern of *c*-sapphire substrate with NS, as shown in Fig. 2(a) to determine the orientation of the sapphire substrate edges. The relative orientation of the NS thereon may be ascertained from SEM data at various magnifications by comparison with the physical sample edges, as shown in Fig. 2(b). The long axes of the NS lie parallel to one of the equivalent  $\langle 10\bar{1}0 \rangle$ -type sapphire in-plane directions.

Despite the similarity of the growth to that used for growth of ZnO nanostructures, CL (voltage 5 kV and current 5 nA) and Raman data (Fig. 3) indicate that the NS are not ZnO material. CL data (Fig. 3(d)) with the electron beam focused both on NS grown at 950 °C and in intervening regions show a broad band at 330 nm (associated with emission from a colour centre defect in sapphire [9]), with a second order replica at longer wavelength settings. Both spectra are very similar, with no evidence of any new peaks due to the NS. The peak emission is reduced when the electron beam is focused on the NS, and there is no evidence of the characteristic band-edge emission due to ZnO at ~380 nm [4]. Micro-Raman spectra on a sample (Fig. 3(e)) partially covered in gold with ZnO material (in the gold-coated portions; region (i)) and NS (in the uncoated portions; region (ii)) are shown in Fig. 3(f). Region (ii) shows no Raman signal from the NS and specifically no signal from the characteristic resonantly enhanced LO modes from ZnO. All the lines in the spectrum can be indexed to the sapphire substrate [10]. We see

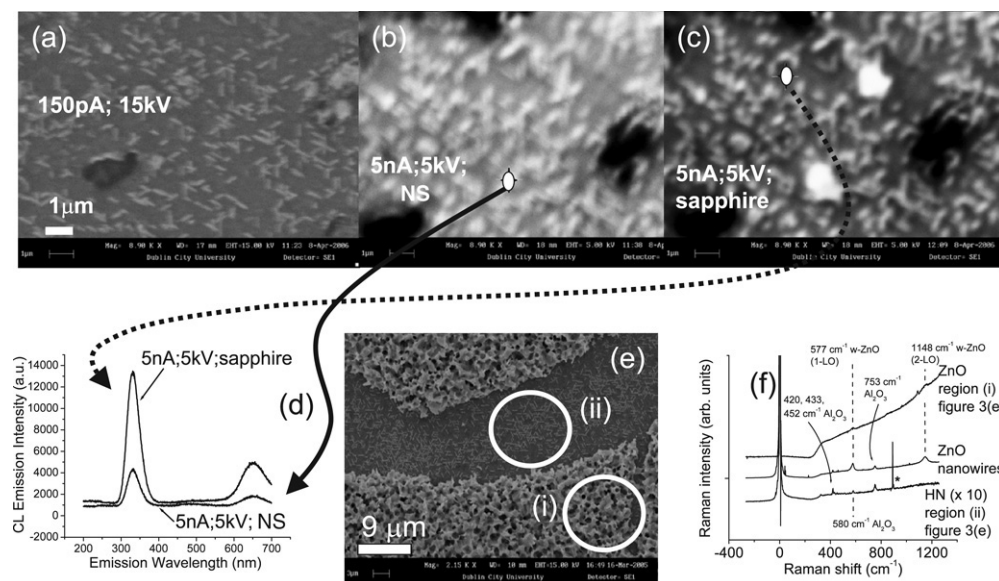


Fig. 3. (a) SEM image at low current and high voltage of region of NS grown at  $\sim 950^\circ\text{C}$ ; (b) & (c) SEM image of same region with same scale at high current and low voltage showing points where the CL spectra of the substrate and NS were obtained (white dots, size indicative of sampled area); (d) CL spectra of the points in figures (b) & (c); (e) SEM image of a sample partially covered in gold with both ZnO and NS (regions (i) and (ii), respectively). Sample grown at  $1125^\circ\text{C}$  for 30 min; (f) Raman data from samples in Fig. 3(e). Asterisk (\*) indicates detector spike.

the ZnO LO modes (on a luminescence background) from region (i) [11]. Fig. 3(f) also shows the Raman signal from a sample containing only ZnO nanowires, grown with gold catalyst, at similar coverage levels to the NS, showing the presence of the ZnO 1-LO and 2-LO modes, in addition to the sapphire signal.

Cross-sectional TEM data are shown in Fig. 4 for a sample grown at  $950^\circ\text{C}$  for 30 min. Part of the region thinned to electron transparency is shown in Fig. 4(a). The substrate is marked at A and two categories of deposit are seen at B and C. A capping layer of gold (from SEM) is seen at D and there is a protective Pt based 'mask' at E (the gold and Pt serve to prevent ion damage of the sample during ion beam thinning). Two types of microstructures are formed: the coarse grained region marked at B ( $\sim 300$  nm in height) and the rather thinner layer at C (varies in thickness from  $\sim 15$  to  $90$  nm). Electron diffraction (Fig. 4(b)) shows that both microstructure types are  $\text{ZnAl}_2\text{O}_4$  phase ( $a_0 = 0.80848$  nm;  $SG : Fd - 3 m$ ). The zinc aluminate phase grows due a reaction between the Zn and O in the vapour and the sapphire substrate ( $\text{Al}_2\text{O}_3$ ) [12]. The grains located in Region C are found to be randomly oriented whereas the thicker grains exhibit a clear orientation relationship with the substrate of the form  $[10\bar{1}0] \text{ Al}_2\text{O}_3 // [011] \text{ ZnAl}_2\text{O}_4$  and  $(0002) \text{ Al}_2\text{O}_3 // (\bar{2}\bar{1}1) \text{ ZnAl}_2\text{O}_4$ . We associate the NS we see in SEM with the coarse grained structures (B) since they are the only fraction which show an epitaxial relationship with the substrate, as suggested by the symmetry of the NS seen in SEM. Their height above the surrounding substrate ( $\sim 70$  nm in this case) is rather similar to that found in AFM. The width of the coarser grains from TEM ( $\sim 390$  nm) is however much larger than the apparent diameters from SEM. In addition, the  $\text{ZnAl}_2\text{O}_4$  NS are surrounded by polycrystalline  $\text{ZnAl}_2\text{O}_4$  so the high contrast, high aspect ratio NS seen in SEM are puzzling. However, the imaging and thus the apparent width in SEM is affected by contrast mechanisms related to edge and other effects. The unusual structure of the

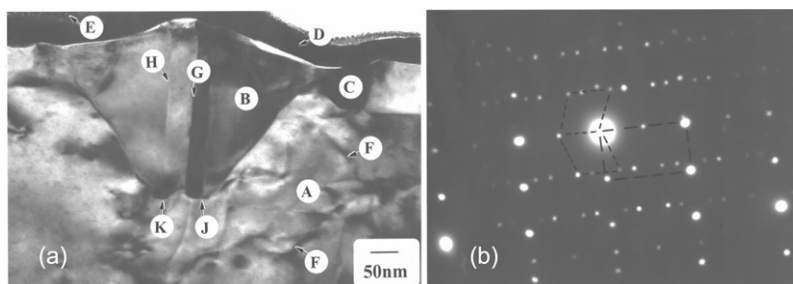


Fig. 4. (a) Cross-sectional TEM image of sample grown at  $\sim 950$  °C, the feature A, B, etc. are discussed in the text; (b) electron diffraction image from coarse grained region B and substrate region of Fig. 4(a) at a sapphire  $[10\bar{1}0]$  zone normal and an aluminate  $[011]$  zone normal.

$\text{ZnAl}_2\text{O}_4$  NS, with evidence in some cases (not shown here) of sharp, faceted tips, and of well defined twin boundaries in all examples (see below) may lead to the narrow diameter, high aspect ratio SEM images we see, due to various contrast effects associated with secondary electron emission. This will be examined in more detail in future work. The substrate defect density is characteristically high, typified by the dislocation at F in Fig. 4(a) and it may be that the structures nucleate at such defects. We note also twin boundaries marked at e.g. H & G in Fig. 4(a), also seen in diffraction (Fig. 4(b)), and the enhanced growth at boundaries J & K. These features and NS nucleation processes will be fully discussed in a future publication.

#### 4. Conclusions

We have demonstrated growth of  $\text{ZnAl}_2\text{O}_4$  NS on *c*-sapphire using VPT. The NS have the appearance in SEM images of high aspect ratio horizontal nanowires with an almost monodisperse diameter distribution, and grow as three equivalent crystallographic variants with the long axis of the NS along the  $\langle 10\bar{1}0 \rangle$ -type substrate in-plane directions. Growth is stable over a range of growth temperatures and durations. Self-organized  $\text{ZnAl}_2\text{O}_4$  NS may have applications in technologies such as sensing and catalysis.

#### Acknowledgements

We acknowledge the support of SFI (Investigator Grant # 02/IN1/I95), the HEA and the EU - Research Infrastructure Action (FP6: "Structuring the European Research Area"). We thank Rolf Simon for help in using the beamline at the ANKA facility of the FZK.

#### References

- [1] S.J. Pearton, D.P. Norton, K. Ip, Y.W. Heo, T. Steiner, *Progr. Mater. Sci.* 50 (2005) 293.
- [2] H.J. Fan, P. Werner, M. Zacharias, *Small* 2 (2006) 700.
- [3] B. Nikoobakht, C.A. Michaels, S.J. Stranick, M.D. Vaudin, *Appl. Phys. Lett.* 85 (2004) 3244.
- [4] J. Grabowska, A. Meaney, K.K. Nanda, J.-P. Mosnier, M.O. Henry, J.-R. Duclère, E. McGlynn, *Phys. Rev. B* 71 (2005) 115439.
- [5] S. Mathur, M. Veith, M. Haas, H. Shen, N. Lecerf, V. Huch, S. Hufner, R. Haberkorn, H.P. Beck, Mohammad Jilavi, *J. Amer. Ceram. Soc.* 84 (2001) 1921.
- [6] S.B. Newcomb, in: S. McVitie, D. McComb (Eds.), *Inst. Phys. Conf. Ser.*, vol. 179, Inst. Phys., Bristol, 2004, p. 357.
- [7] R. Rantamaki, T. Tuomi, Z.R. Zytewicz, P.J. McNally, A.N. Danilewsky, *J. X-ray Sci. Technol.* 8 (2000) 277.
- [8] <http://www.ccp14.ac.uk/ccp/web-mirrors/lmgp-laugier-bochu/>.

- [9] B.D. Evans, G.J. Pogatshnik, Y. Chen, Nucl. Instrum. Methods B 91 (1994) 258.
- [10] E. Zounoulis, D. Renusch, M. Grimsditch, Appl. Phys. Lett. 72 (1998) 1.
- [11] J.F. Scott, Phys. Rev. B 2 (1970) 1209.
- [12] C.R. Gorla, W.E. Mayo, S. Liang, Y. Lu, J. Appl. Phys. 87 (2000) 3736.